Article

Reaction of Glycerol with Trimethyl Orthoformate: Towards the Synthesis of New Glycerol Derivatives

Roberto Calmanti, Emanuele Amadio[ID]**, Alvise Perosa ***[ID] **and Maurizio Selva ***[ID]

Department of Molecular Sciences and Nanosystems, Università Ca' Foscari Venezia, Via Torino 155,
30172 Venezia Mestre, Italy; roberto.calmanti@unive.it (R.C.); emanuele.amadio@unive.it (E.A.)
* Correspondence: alvise@unive.it (A.P.); selva@unive.it (M.S.);
   Tel.: +39-041-234-8958 (A.P.); +39-041-234-8687 (M.S.)

check for
updates

Abstract: The reactivity of glycerol with trimethyl orthoformate is here described with an emphasis on developing a reliable synthetic approach for glycerol valorization. The glycerol based orthoester 4-(dimethoxymethoxy)methyl)-2-methoxy-1,3-dioxolane (**3**) was synthesized, under catalytic as well as catalyst-free conditions, by taking advantage of the thermodynamically controlled equilibrium between intermediates. Both Brønsted and Lewis acid catalysts accelerated the attainment of such an equilibrium, particularly Brønsted acidic ionic liquids BSMImHSO$_4$ and BSMImBr were the most effective compounds for this reaction. The kinetic profiles allowed the proposal of a mechanism that accounts for the selectivity of the reaction.

Keywords: glycerol; orthoesters; Brønsted acid; ionic liquids; trimethyl orthoformate

---

1. Introduction

Glycerol (Glyc) is one of the most important biomass-derived platform chemicals [1]. Over the last few decades, the overabundance of this bio-diesel by-product stimulated academic and industrial interests towards its conversion into renewable high value-added chemicals [2–7]. Some of the most promising processes are summarized in Figure 1.

In this field, our research group has explored different thermal and catalytic synthetic approaches by reacting Glyc with formaldehyde, acetone, dimethyl carbonate, and enol esters to yield acetals, ketals, and other sustainable derivatives [8–13]. In a search to further expand this chemistry and to identify new bio-building blocks, we considered orthoesters (OEs) as another family of electrophilic partners for the upgrading of Glyc.

The impressive reactivity of OEs—up to 20,000 times higher than of the above cited ketones and aldehydes [14]—has stimulated significant studies for their applications as protecting groups for carboxylic acids and esters [15] (owing to their stability towards strong nucleophiles and bases), as dehydrating agents [16,17], and as copolymers for the synthesis of polyorthoesters [18,19]. More recently, a fascinating use of OEs in the synthesis of dynamic cryptands has been proposed, employed for the controlled release of metal ion guests [20,21].
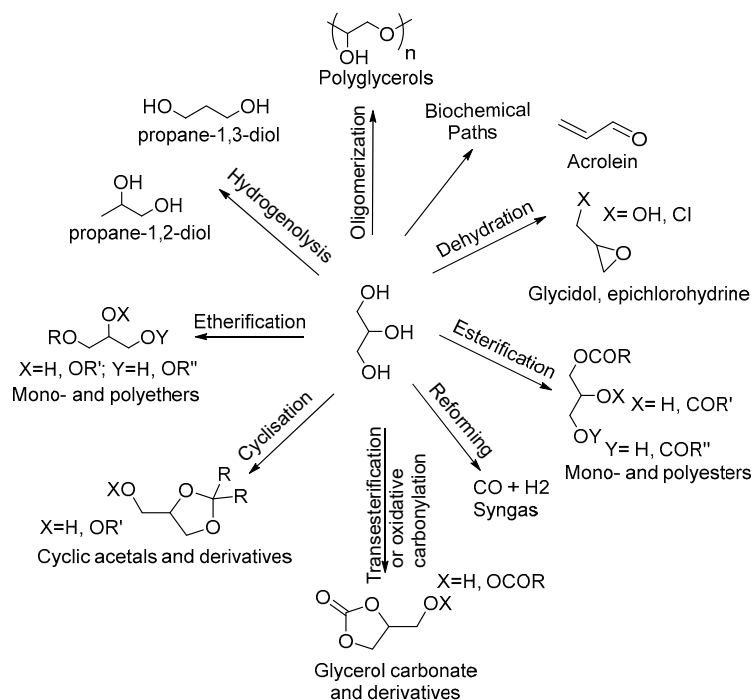
Figure 1. Glycerol conversion routes.

Some pioneering research dating back to the '60s and '80s highlighted the potential of the reaction of Glyc with OEs. In 1964, Crank and Eastwood were the first to investigate the reaction between triols and triethylorthoformate to obtain bicyclic orthoesters (BOEs) [22], demonstrating the formation of several BOEs from 1,2,4- 1,2,5- and 1,3,5-triols. By using Glyc as reagent, they observed the formation of a mixture of the pentacyclic *cis-/trans*-2-ethoxy-4-hydroxymethyl-1,3-dioxolane (**1**) and its hexacyclic isomer *cis-/trans*-2-ethoxy-5-hydroxy-1,3-dioxane (**4**) (Figure 2a) in a 9:1 ratio with 67% of yield, which could thermally decomposed to ethanol, CO_2 and allyl alcohol [23]. The bicyclic compound 2,6,7-trioxabyciclo [2.2.1] heptane (**2**) was not observed. A few years ago, Thshibalonza and Monbaliu revisited the reaction by focusing on the formic acid-catalyzed synthesis of allyl alcohol under continuous-flow conditions (Figure 2b) [24].

In the late 1970s, Hall et al. successfully accomplished the synthesis of **2** (Figure 2c, Yield ≈ 70%) and its further polymerization to five-membered rings polyorthoesters [25,26]. Since then, the ring-opening polymerizations of BOEs (including **2**) have been extensively investigated and reviewed [27–29].

Furthermore, diglycerol-OEs were used also to develop acid-labile polymers for drug-delivery applications [18,30].

In this work, the thermal and catalytic reaction between Gly and $HC(OMe)_3$ is studied with the aim to develop new reliable synthetic protocols for glycerol exploitation. The selective formation (up to 95% of yield) of a new glycerol-based 5-membered ring di-orthoester (the *cis-/trans*-4-(dimethoxymethoxy)methyl)-2-methoxy-1,3-dioxolane; **3**, Figure 2d) was accomplished by using $HC(OMe)_3$ as model OE via a dynamic and thermodynamically-controlled synthetic strategy. A variety of homogeneous and heterogeneous acids (PPTS, DBUHBr, sulfuric acid, Amberlyst-15, amberlyst-36, $FeCl_3$, and AlF_3) and ionic liquids (BSMImHSO$_4$, BSMImBr) were used as Brønsted/Lewis-acidic catalysts. In this context, the ionic liquids (ILs) were tested as they are known to give better yields, turnover numbers, and frequencies, and improved catalysts recyclability [31]. The effect of basic catalysts (such as K_2CO_3 and trioctylmethylphosphonium methylcarbonate: $[P_{1888}]CH_3OCO_2^-$) was also investigated for comparison.
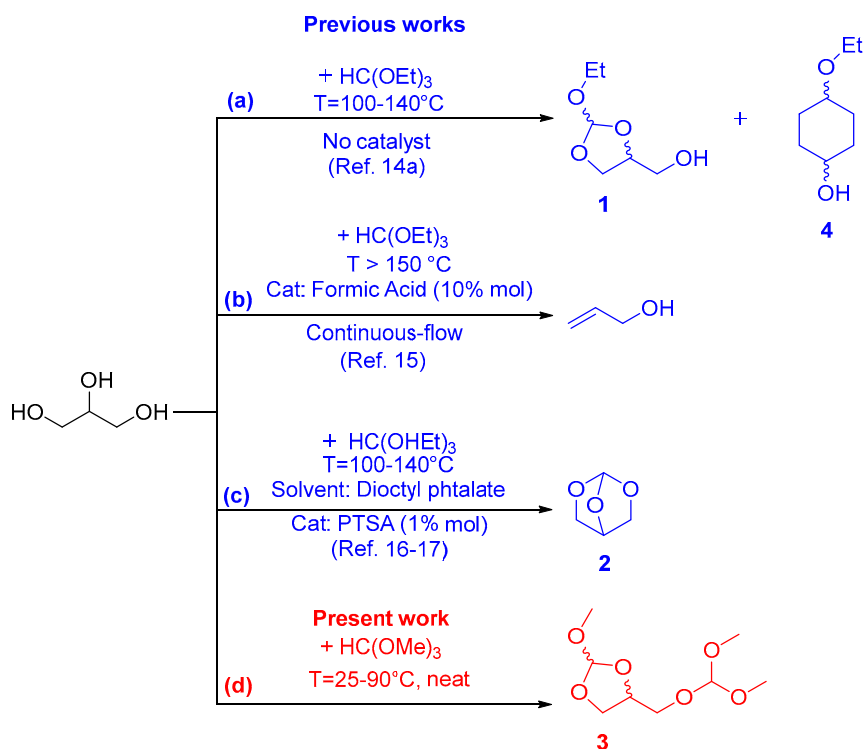
**Figure 2.** Reactions between Gly and OEs.

2. Results and Discussion

The reactivity between Glyc and HC(OMe)$_3$ was first tested in the absence of any catalyst, in analogy to the reaction conditions previously reported in literature [22,25,26]. The reaction was carried out in the absence of added solvents at 90 °C with a reagent molar ratio Q = 1 (Q = HC(OMe)$_3$:Glyc) for 1 h. The products were isolated and fully characterized by GC-MS, ^{1}H, ^{13}C, and 2D-NMR analyses (see Material and Methods or Supplementary Materials for further details) revealing the formation of the five-membered ring OE **1**, the bicyclic compound 2,6,7-trioxabyciclo [2.2.1] heptane **2**, and the di-orthoester **3** (**1** and **3** as mixtures of diastereomers) in 82/11/7 selectivity respectively (Figure 3). Figure 4 shows the gaschromatogram of the crude reaction mixture.
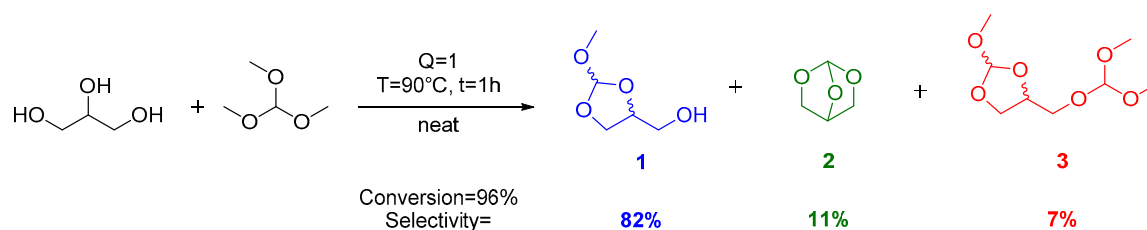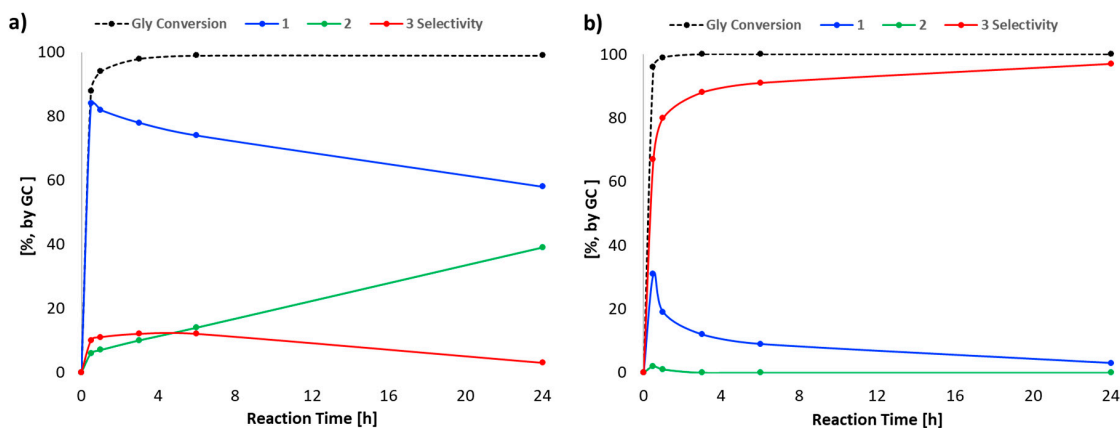

Figure 3. Reaction of Gly with HC(OMe)$_3$.

The six-membered ring isomers **4** and the correspondent **3** derivative were not observed. This was unexpected, since previous results for the reaction between Glyc and triethyl orthoformate reported a five- and six-membered ring isomeric ratio of 3:1 [26] or 9:1 [22] for compounds **1:4**. A reasonable explanation is that, under our conditions, the reaction between glycerol and HC(OMe)$_3$ is kinetically rather than thermodynamically controlled. Indeed, the ring strain energy of five-membered ring 1,3-dioxolane (7.3 kcal/mol) is higher than the six-membered ring 1,3-dioxane analogs (2.9 kcal/mol) [32], while the stabilization energy due to their formation was 4.4 and 13.2 respectively [33]. These trends of energies show that 1,3-dioxane are more stable than 1,3-dioxolane. This explanation is also in

agreement with the results reported by Yokohama et al. for the ring-opening polymerization of **2** that under kinetical control, leads to the almost exclusive formation of the five-membered ring product [26].
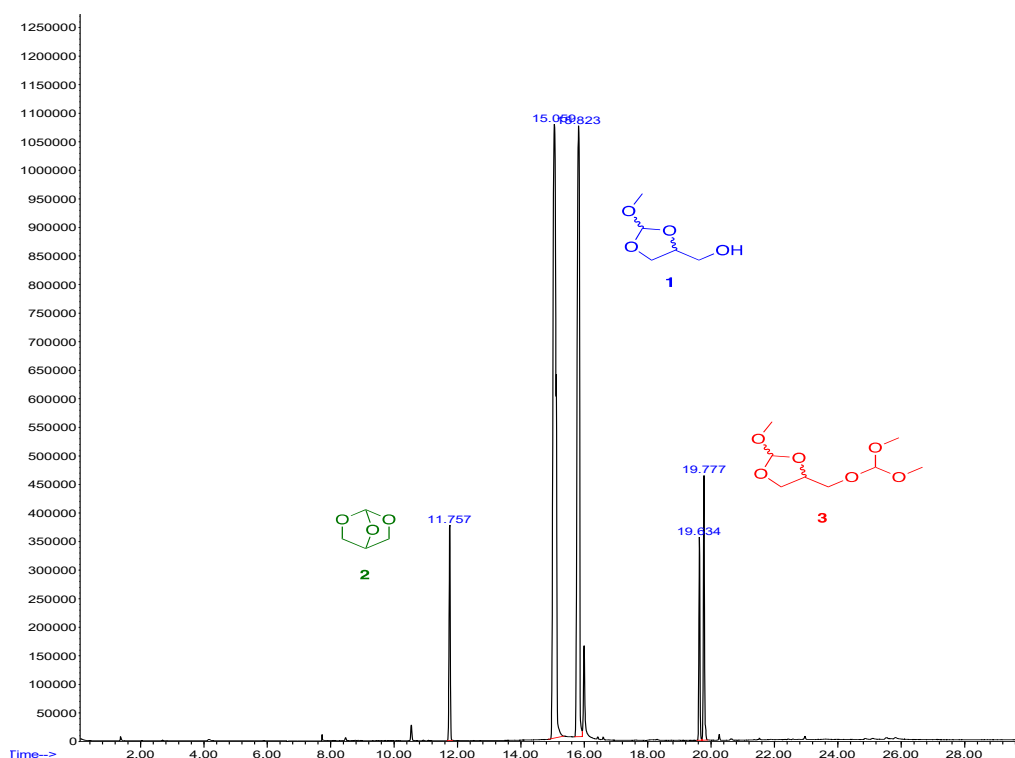

Figure 4. Gaschromatogram of the reaction between $HC(OMe)_3$ and Gly with Q = 1, 90 °C, 1 h.

Further experiments were then carried out at different temperatures and Glyc:$HC(OMe)_3$ molar ratios by following the product distribution over the time. At 90 °C, under reactive distillation conditions to remove methanol continuously during the reaction, the kinetic profile of the reaction was studied for 24 h at two different molar ratios Q = 1 and Q = 10 (Figure 5a,b). In both cases, within the first minutes of reaction the initial biphasic mixture turned homogeneous and vigorous distillation of methanol was observed. For both ratios Q = 1 and Q = 10, the Glyc conversion was almost quantitative after 0.5 h (based on GC analysis) towards formation of **1** and **3** respectively, thus proving that the formation of the glycerol-OEs is basically instantaneous, yielding a statistical product distribution. After 24 h, a relatively slow dynamic covalent exchange reaction yielded a thermodynamically controlled product distribution which is influenced by the reaction conditions. For example, with Q = 1, after 1 h the selectivity was shifted towards **1**, but prolonging the reaction time, **1** and **3** slowly decreased in favor of the formation of **2** (39% after 24 h) via an intramolecular reaction favored by the continuous removal of methanol. When using an excess of $HC(OMe)_3$ (Q = 10) the initial selectivity was shifted towards the formation of **3** (80%, 1 h), as expected; after 24 h the reaction slowly proceeded further favoring conversion of **1** into **3** (97%, 24 h). It is worth noting that, under these conditions, **3** could be isolated by simply evaporating the excess of $HC(OMe)_3$ without any further purification step (95% isolated yield with 98% purity by GC).

Figure 5. Conversion of Gly and products selectivity for the catalyst-free reaction between Gly and HC(OMe)$_3$. Reaction conditions: Gly [5.43 mmol] and HC(OMe)$_3$ with Q = 1 (**a**) or Q = 10 (**b**) at 90 °C.

The experimental results indicated that—likewise to the known glycerol-orthoformate reactivity [22–24,26] and the alkoxy-exchange reactivity of OEs [34]—the initial fast reaction of HC(OMe)$_3$ with Glyc gives **1** which is in equilibrium with **2** and **3**, the latter formed by reaction with another molecule of orthoformate. Interconversion of **2** and **3** goes through a dynamic covalent reaction involving **1** as the intermediate. Scheme 1 shows the hypothesized reaction pathways.
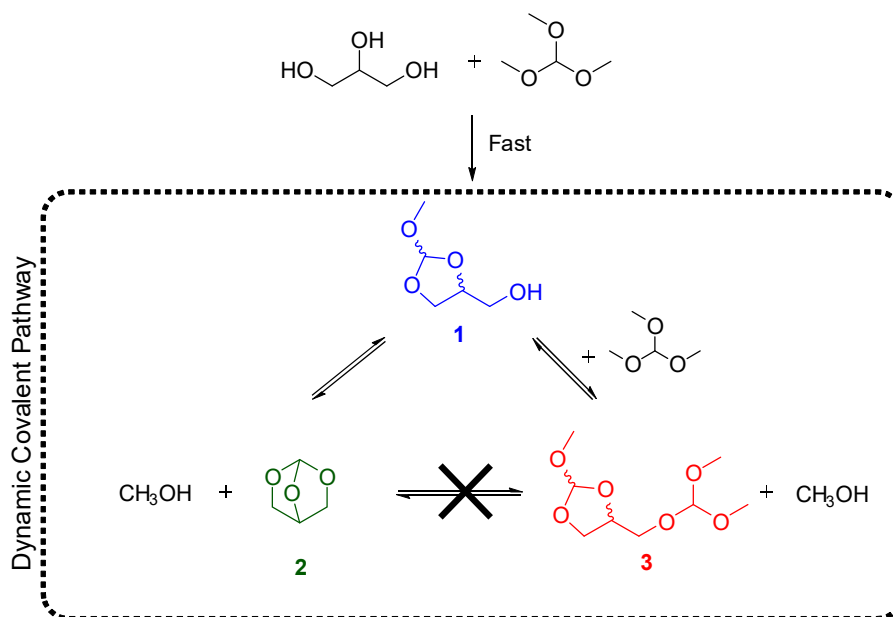
Scheme 1. Pathways for the Gly and HC(OMe)$_3$ reaction.

The reaction was further investigated by varying Q between 1 and 10, at T = 90 °C and 25 °C, for 24 h. As shown in Table 1, **3** was formed selectively at 90 °C only with a large excess of HC(OMe)$_3$ (Q = 10) (entry 5, Table 1). At lower Q values instead (entries 1–4, Table 1), the selectivity-determining dynamic equilibrium resulted in a statistical products distribution.

Table 1. Q and T effect on products distribution for the catalyst-free reaction of Gly with HC(OMe).
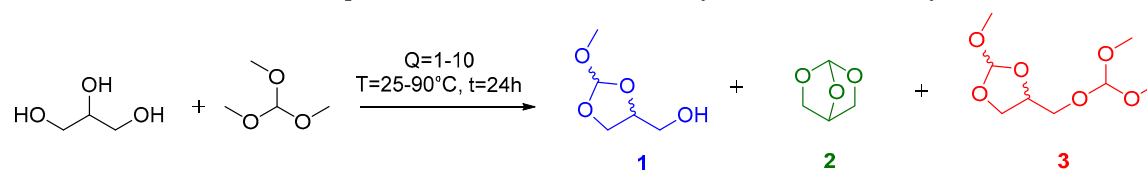
Entry	Q	T (°C)	Conversion (%) [a]	Selectivity (%) [a]		
				1	**2**	**3**
1	1	90	96	58	39	3
2	1.5	90	96	56	9	35
3	2	90	96	51	3	46
4	5	90	99	24	2	74
5	10	90	100	3	0	97
6	1	25	63	79	8	13
7	10	25	95	74	5	21

Reaction conditions: Gly (5.43 mmol) and HC(OMe)$_3$ with Q = 1–10, T = 90 °C, t = 24 h. [a] Conversion of Gly and products selectivity determined by GC.

A less pronounced exchange equilibrium between the products was observed for the reactions conducted at 25 °C respect to the ones conducted at 90 °C. In fact, at 25 °C and Q = 1 the reaction was very slow and after 24 h, conversion reached only 63% (90% conversion after 48 h), with 79% selectivity towards formation of **1** (entry 6, Table 1 and Figure S32 for the reaction profile). At higher Q = 10, the reaction rate increased reaching almost quantitative conversion, but the product distribution was not shifted towards the formation of **3**, as was the case for the reaction conducted at 90 °C. Instead, a high (88%) selectivity towards **1** was observed after 1 h, while after 24 h the dynamic equilibrium promoted a 74/5/21 selectivity towards **1/2/3** respectively (entry 7 and Figure S33 for the reaction profile).

Overall, the catalyst-free reaction between Gly and HC(OMe)$_3$ lead to the selective synthesis of the thermodynamically-favored product **3**—a new orthoester derivative of glycerol—after 24 h and in the presence of an excess of OE.

With the aim to accelerate attainment of the dynamic equilibrium among **1**, **2**, and **3**, and to direct selectivity, different acid catalysts were then tested at Q = 10 and T = 90 °C. The results are listed in Table 2. In the presence of PPTS (10%w/w$_{gly}$), known to catalyze the reaction of diglycerol with triethyl orthoformate [30], the reaction reached quantitative conversion and 97% selectivity towards **3** in 1 h (entries 3 and 4; Table 2). No further products were observed even after 24 h, indicating that **3** is stable under the reaction conditions (Figure S34 for the reaction profile). As shown in Table 2, all the other acid catalysts favored the formation of **3** already after 1 h. Only for diazabicyclo-undecenium bromide (DBUHBr, entries 5 and 6, Table 2) a slower dynamic equilibrium—in line with the uncatalyzed reaction—was observed (75% and 93% selectivity after 1 and 24 h, respectively) likely due to the lower acidity [35]. Brønsted and Lewis acidic catalysts such as H$_2$SO$_4$, amberlyst-15, amberlyst-36, iron chloride and aluminum fluoride promoted moderate-to-good selectivity (84%, 79%, 87%, 91%, 87%, respectively; entries 7, 9, 11, 13, 15, Table 2) towards **3** after 1 h along with small amount of ill-defined products (e.g., aldehydes, ethers, or oligomers). The latter were probably formed by catalytic decomposition of **3** as already described in the literature for OEs [26,36,37]. The reaction became evident after 24 h. In particular, the use of sulfuric acid caused formation of a large quantity (≈41%) of four major undefined products (see Figures S35–S39 for the gas-chromatography trace and MS spectra) after 24 h at 90 °C. Instead, when using the ionic liquids butylsulfonylmethylimidazolium bromide (BSMImBr) and hydrogensulfate (BSMImHSO$_4$) as catalyst (entries 17–20, Table 2) the fast reaction rates were always accompanied by the quantitative and selective formation of **3** (98%) and by the absence of side reactions (99% also after 24 h). The same acidic ionic liquids allowed to perform the reaction at 25 °C, still with appreciable selectivity towards **3** (81–87%; entries 21–22; Table 2). Finally, no

conversion of Glyc was observed when using basic catalysts, such as K_2CO_3 or $[P_{1888}]CH_3OCO_2^-$ [38], owing to the stability of OEs towards bases.

To rationalize the catalytic behavior, the Hammett acidity functions (H_0) for the different catalysts were compared (see Table 2). H_0 was chosen as it is one of the most effective ways to express the Brønsted acidity in an organic medium [39,40]. It is readily apparent that stronger acidity ($H_0 < 0$, entries 7–12) prompts faster reactions but also higher formation of side products. On the other hand, when using weaker acids ($H_0 = 1–3$, entries 17–22) the reactions are more selective towards the formation of the desired product **3**.

Table 2. Catalyzed reaction between $HC(OMe)_3$ and Gly.
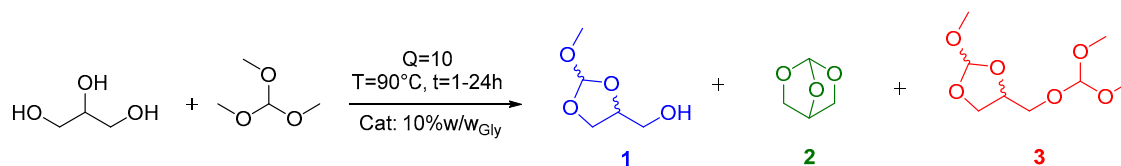
Entry	Catalyst	Time (h)	Conversion (%) [a]	Selectivity (%) [a]				H_0 [b]
				1	2	3	Others	
1	—	1	96	19	1	80	-	
2	—	24	>99	3	0	97	-	
3	PPTS	1	>99	0	3	97	-	
4	PPTS	24	>99	0	3	97	-	
5	DBUHBr	1	96	25	0	75	-	
6	DBUHBr	24	>99	7	0	93	-	
7	H_2SO_4	1	>99	9	2	84	5	−12.3 [41]
8	H_2SO_4	24	>99	42	1	16	41	
9	A-15	1	>99	12	3	79	6	−2.2 [42,43]
10	A-15	24	>99	17	1	70	12	
11	A-36	1	>99	7	1	87	5	−2.65 [42,43]
12	A-36	24	>99	13	1	75	11	
13	$FeCl_3$	1	>99	2	0	91	7	
14	$FeCl_3$	24	>99	10	1	78	11	
15	AlF_3	1	>99	9	1	87	3	
16	AlF_3	24	>99	3	1	92	4	
17	BSMImHSO$_4$	1	>99	0	2	98	-	1.02 [44]
18	BSMImHSO$_4$	24	>99	0	1	99	-	
19	BSMImBr	1	>99	0	2	98	-	2.91 [c] [45]
20	BSMImBr	24	>99	0	1	99	-	
21	BSMImHSO$_4$ [d]	1	>99	17	2	81	-	
22	BSMImBr [d]	1	>99	11	2	87	-	
23	K_2CO_3	1	0	0	0	0	-	
24	$[P_{1888}]CH_3OCO_2^-$	1	0	0	0	0	-	

Reaction conditions: Gly (5.43 mmol) and $HC(OMe)_3$ with Q = 10, 10%$_{w/w\ Gly}$ of catalyst, 90 °C, 1–24 h. [a] Conversion of Gly and products selectivity determined by GC. [b] Hammett acidity function according to literature data. [c] the value reported was calculated for butylsulfonylmethylimidazolium chloride. [d] The reaction was carried out at T = 25 °C.

3. Materials and Methods

3.1. General Information

All the chemicals were purchased from Aldrich and used as received. Trioctylmethylphosphonium methylcarbonate ($[P_{1888}]CH_3OCO_2^-$) was synthesized according to a literature procedure [38].

GC analyses were run using a Perkin Elmer Elite-624 capillary column (L = 30 m, Ø = 0.32 mm, film thickness = 1.8 μm). The following conditions were used. Carrier gas: N2; flow rate: 3.5 mL min^{-1}; split ratio: 1:1; initial T: 50 °C (4 min), ramp rate: 10 °C min^{-1}; final T: 180 °C; ramp rate: 20 °C min, final T: 240 °C (10 min). GC-MS (EI, 70 eV) analyses were run using a Grace AT-624 capillary column (L = 30 m, Ø = 0.32 mm, film thickness = 1.8 μm). The following conditions were used. Carrier

gas: He; flow rate: 1.2 mL min^{-1}; split ratio: 10:1; initial T: 50 °C (4 min), ramp rate: 10 °C min^{-1} to 180 °C; ramp rate: 20 °C min, final T: 240 °C (10 min). ^{1}H, ^{13}C{^{1}H}, DEPT-135, DEPT-90, APT, NOESY, HSQC, HMBC, COSY NMR spectra were recorded on a Bruker 400 MHz (^{1}H: 400 MHz; ^{13}C: 100 MHz) spectrometer. For ^{1}H and ^{13}C{^{1}H} NMR the chemical shifts (δ) have been reported in parts per million (ppm) relative to the residual undeuterated solvent as an internal reference.

3.2. Synthesis/Isolation of Reaction Products

3.2.1. Synthesis of (2-methoxy-1,3-dioxolan-4-yl) Methanol (**1**)

Glycerol (5.12 g, 55.6 mmol) was added in a two-neck round bottom flask equipped with a dripping funnel and a heating condenser held at 70 °C. The flask was heated at 90 °C and HC(OMe)$_3$ (6.1 mL, 55.6 mmol) was added dropwise under stirring and kept for 1 h. In Figure 5, the gaschromatographic trace of the reaction crude is reported, highlighting the presence of diastereomers. The reaction mixture was then distilled over potassium carbonate three times to isolate one pure distereoisomer of **1** in 10% yield, hereafter identified as **1a** (the peaks with retention time 15.0 min in Figure 4). The characterization of the other diastereoisomer **1b** (retention time 15.8 min) is inferred from the spectra of the mixture.

^{1}H NMR (400 MHz, Acetone)**1a**: δ = 5.72 (s, 1H), 4.23–4.18 (m, 1H), 4.11–4.04 (m, 1H), 3.84–3.78 (m, 1H), 3.66 (ddd, *J* = 6.0, 5.2, 2.7, 2H), 3.26 (s, 3H). ^{13}C NMR (101 MHz, Acetone) δ = 115.93, 77.03, 65.47, 62.86, 50.22. GC-MS: 134 (M$^+$,0);133 (1); 103 (100); 61 (31); 57 (46); 47 (15); 45 (32); 44 (31); 43 (65). **1b**: 5.73 (s, 1H), 4.32 (ddt, *J* = 6.9, 5.6, 5.0, 1H), 4.11–4.04 (m, 1H), 3.84–3.78 (m, 1H), 3.57 (dd, *J* = 6.0, 5.0, 2H), 3.23 (s, 3H). ^{13}C NMR (101 MHz, Acetone) δ = 115.82, 76.09, 65.42, 62.22, 50.00. GC-MS: 134 (M$^+$,0);133 (1); 103 (100); 74 (8); 61 (18); 57 (47); 47 (15); 45 (28); 44 (14); 43 (46). All the ^{1}H, ^{13}C, COSY, HMBC, HSQC, COSY NMR and the GC-MS spectra are reported in Figures S1–S12.

3.2.2. Synthesis of 2,6,7-Trioxabyciclo [2.2.1] Heptane (**2**)

Any attempt to isolate **2** from the crude reaction mixture proved unsuccessful and it was identified only by GC-MS (Figure S13). GC-MS: 102 (M$^+$,8);101 (4); 45 (15); 44 (100); 43 (62); 42 (6).

3.2.3. Synthesis of 4-(Dimethoxymethoxy)Methyl)-2-Methoxy-1,3-Dioxolane (**3**)

Glycerol (0.526 g, 5.71 mmol) and HC(OMe)$_3$ (6.3 mL, 57.2 mmol) were added in a round-bottomed flask and the mixture was stirred at 90 °C. During the reaction the methanol was distilled out the mixture by heating the condenser at 70 °C. After 24 h the mixture was cooled down and then concentrated under vacuum (60 °C, 35 mbar). **3** was obtained a mixture of two diastereomers in 95% yield without any further purification (purity 98% by GC). The diastereoisomeric ratio of **3** was 1:1 according to GC and ^{1}H NMR analyses (Figure S16). Any attempts to separate the two isomers (hereafter called **3a** or **3b**) failed. ^{1}H NMR (400 MHz, Acetone) **3a** + **3b**: δ = 5.76 (s, 1H), 5.73 (s, 1H), 5.11 (s, 1H), 5.10 (s, 1H), 4.44 (dq, *J* = 6.9, 5.3, 1H), 4.34–4.27 (m, 1H), 4.11 (ddd, *J* = 7.9, 6.8, 5.6, 2H), 3.81–3.77 (m, 2H), 3.71 (dd, *J* = 10.6, 6.1, 1H), 3.65–3.61 (m, 1H), 3.57 (dd, *J* = 6.2, 5.3, 2H), 3.31–3.29 (m, 12H), 3.26 (s, 3H), 3.25 (s, 3H). ^{13}C NMR (101 MHz, Acetone) δ = 116.13, 115.86, 113.99, 113.95, 74.80, 74.11, 66.00, 65.68, 64.82, 63.80 (d, *J* = 2.1), 50.72, 50.71, 50.21, 50.04. GC-MS: 3a: 208 (M$^+$,0);131 (1); 117 (8); 103 (12); 75 (100); 61 (13); 57 (25); 47 (11); 43(9). 3b: 208 (M$^+$,0);131 (2); 117 (8); 103 (12); 75 (100); 61 (13); 57 (25); 47 (11); 45(6); 43 (9). Further discussion on the structural characterization and the ^{1}H, ^{13}C{^{1}H}, DEPT-135, DEPT-90, APT, NOESY, HSQC, HMBC and COSY NMR and GC-MS spectra (Figure S14–S24) are reported in Supporting Information.

3.3. Synthesis of the Acidic Catalysts

3.3.1. Synthesis of Pyridinium Para-Toluensulfonate (PPTS)

The synthesis was carried out following a literature procedure [46]. ^{1}H NMR (400 MHz, MeOD) δ = 8.89 (dt, *J* = 5.2, 1.6, 2H), 8.68 (tt, *J* = 7.9, 1.6, 1H), 8.16–8.09 (m, 2H), 7.75–7.69 (m, 2H), 7.27–7.22 (m, 2H), 2.38 (s, 3H). The spectrum is in agreement with the literature (Figure S25).

3.3.2. Synthesis of Diazobicycloundecenium Bromide (DBUHBr)

An aqueous solution of hydrobromic acid (40% v/v, 13.2 mmol) was dripped into a vessel containing an equimolar amount of DBU under continuous stirring. After 24 h, the aqueous solution was concentrated by rotary evaporation (60 °C, 40 mbar) and any trace of water was removed under reduced pressure (60 °C, 1 mbar) until a white solid was obtained (yield = 99%). ^{1}H NMR (400 MHz, D_2O) δ = 3.50 (dt, *J* = 18.0, 5.6, 4H), 3.28 (t, *J* = 5.9, 2H), 2.62–2.55 (m, 2H), 1.97 (tt, *J* = 7.2, 5.2, 2H), 1.74–1.60 (m, 6H). ^{13}C NMR (101 MHz, D_2O) δ = 165.95, 54.19, 48.26, 38.01, 32.87, 28.47, 25.90, 23.34, 18.96. (Figures S26 and S27).

3.3.3. Synthesis of Butylsulfonylmethylimidazolium Hydrogensulfate (BSMImHSO$_4$)

1-methylimidazole and 1,4-butane-sultone were charged into a 100 mol round-bottom flask in an equimolar amount (0.1 mol) and stirred at 80 °C for 16 h. The white solid zwitterionic product was washed with ethyl ether (10 × 5 mL) to remove any unreacted starting materials and the solid was dried in vacuum. Then, a stoichiometric amount of sulfuric acid (95% v/v H_2O) was added and the mixture stirred at 60 °C for 10 h, to obtain the ionic liquid BSMImHSO$_4$. The IL was washed again with dichloromethane and ether and dried under vacuum. BSMImHSO$_4$ was obtained in 95% of yield and it was used without any further purification. ^{1}H NMR (400 MHz, D_2O) δ = 8.61 (s, 1H), 7.38 (s, 1H), 7.31 (s, 1H), 4.11 (s, 2H), 3.77 (s, 3H), 2.82 (s, 2H), 1.88 (s, 2H), 1.62 (s, 2H). ^{13}C NMR (101 MHz, D_2O) δ = 135.90, 123.60, 122.11, 50.01, 48.86, 35.61, 28.04, 20.87. All spectra (Figures S28 and S29) are in agreement with those reported in literature [40].

3.3.4. Synthesis of Butylsulfonylmethylimidazolium Bromide (BSMImBr)

1-methylimidazole and 1,4-butane-sultone were charged into a 100 mol round-bottom flask in an equimolar amount (0.1 mol) and stirred at 80 °C for 16 h. The white solid zwitterionic product was washed with ethyl ether (10 × 5 mL) and dried in vacuum (yield = 90%). Then a stoichiometric amount of hydrobromic acid (40% v/v H_2O) was added and the mixture stirred at 60 °C for 10 h to yield to the ionic liquid BSMImBr. The ionic liquid (IL) was washed again with dichloromethane and ether to remove non-ionic residues and dried under vacuum. The IL was obtained with a 90% yield and used without any further purification. ^{1}H NMR (400 MHz, D_2O) δ = 8.66–8.61 (m, 1H), 7.40 (t, *J* = 1.8, 1H), 7.34 (t, *J* = 1.8, 1H), 4.15 (t, *J* = 7.0, 2H), 3.79 (d, *J* = 0.6, 3H), 2.87–2.81 (m, 2H), 1.97–1.87 (m, 2H), 1.68–1.58 (m, 2H). ^{13}C NMR (101 MHz, D_2O) δ = 135.92, 123.63, 122.14, 50.04, 48.90, 35.68, 28.08, 20.90. (Figures S30 and S31)

3.4. General Procedures for the Gly-HC(OMe)$_3$ Reactions

3.4.1. Catalyst-Free Conditions

Glycerol (0.5 g, 5.43 mmol) and cyclopentyl methyl ether (100 μL) as an internal standard were added in a two-neck round-bottomed flask equipped with a dripping funnel and a condenser. The mixture was stirred at the selected temperature (T = 25 or 90 °C) and HC(OMe)$_3$ was added dropwise by varying the molar ratio Q from 1 to 10. The reaction was allowed to proceed for 24 h under stirring and samples were collected and analyzed by GC at regular intervals. For reactions run at 90 °C, the condenser was heated at 70 °C in order to continuously distill methanol.

3.4.2. Catalyzed Reaction

The above reported procedure was followed with the exception that the selected catalyst (10% w/w_{Gly}) was added with glycerol and cyclopentyl methyl ether, before the addition of $HC(OMe)_3$.

3.4.3. Catalytic Procedure for the Synthesis of **3**

Glycerol (0.5 g, 5.43 mmol), $HC(OMe)_3$ (5.9 mL, 54.3 mmol) and a catalytic amount of the selected catalyst (BSMImHSO$_4$, BSMImBr, 3% mol/mol$_{gly}$) were added in a round-bottomed flask and the mixture was stirred at 90 °C. During the reaction the methanol was distilled out the mixture by heating the condenser at 70 °C. After 1h, the mixture was cooled down and the solution was passed through a short plug of alumina. The filtered solution was concentrated under vacuum (60 °C, 35 mbar). **3** was obtained as a mixture of two diastereomers in 96% yield without any further purification (purity 98% by GC).

4. Conclusions

The thermal and catalytic reactivity of glycerol with trimethyl orthoformate was fully explored here for the first time.

Under catalyst-free conditions, with an equimolar mixture of Gly and $HC(OMe)_3$ (Q = 1), the reaction leads to the unselective formation of a dynamic equilibrium mixture of products **1**, **2**, and **3** (Scheme 1 and Table 1). The products were isolated and fully characterized by GC-MS, ^1H, ^{13}C, and 2D-NMR spectroscopy revealing the formation exclusively of the five-membered ring isomers of **1** and **3**, obtained as mixtures of two diastereoisomers. The equilibrium of this reaction is remarkably shifted towards the formation of **3** as evinced for longer reaction times, higher temperature and/or using a large excess of orthoformate (Q = 10). **3** could thus be obtained selectively in high yields at 90 °C with 10 equivalents of trimethyl orthoformate after 24 h.

Both the reaction time and temperature can be reduced by using Brønsted and Lewis-acid catalysts. The strongest acidic catalysts (H_2SO_4, A-15, A-36, iron chloride, and aluminium fluoride) accelerate attainment of the dynamic equilibrium of the reaction to yield preferentially **3**, but also promote ill-defined degradation products. Less acidic catalysts such as the ionic liquids BSMImHSO$_4$ and BSMImBr also accelerate attainment of the thermodynamically favored product **3** (98–99%) without however further degradations as indicated by the stability of **3** over time.

Overall, the present results shed light on the reaction pathway and on the equilibria that govern conversion of glycerol into its orthoesters **1** and **3** and it allows to selectively synthesize **3** by a proper choice of reaction conditions. The glycerol-based orthoesters represent new building blocks en route to the development of more complex glycerol-OEs architectures.

Supplementary Materials: The following are available online at http://www.mdpi.com/2073-4344/9/6/534/s1, GC-MS chromatograms, NMR spectra and reaction profiles. Figure S1: MS spectra of 1a. Figure S2: ^1H NMR of 1a. Figure S3: $^{13}C\{^1H\}$ NMR of 1a. Figure S4: HSQC spectra 1a. Figure S5: HMBC spectra of 1a. Figure S6: COSY spectra of 1a. Figure S7: MS spectra 1b. Figure S8: ^1H NMR of 1a,b. Figure S9: $^{13}C\{^1H\}$ NMR of 1a,b. Figure S10: HSQC of 1a,b. Figure S11: HMQC of 1a,b. Figure S12: COSY of 1a,b. Figure S13: GC-MS spectra of 2. Figure S14: MS spectra of 3a. Figure S15: MS spectra of 3b. Figure S16: ^1H NMR of 3a,b. Figure S17: $^{13}C\{^1H\}$ NMR of 3a,b. Figure S18: DEPT-135 of 3a,b. Figure S19: DEPT-90 of 3a,b. Figure S20: ATP of 3a,b. Figure S21: COSY of 3a,b. Figure S22: HMBC of 3a,b. Figure S23: HSQC of 3a,b. Figure S24: NOESY of 3a,b. Figure S25: ^1H NMR of PPTS. Figure S26: ^1H NMR of DBUHBr. Figure S27: $^{13}C\{^1H\}$ NMR of DBUHBr. Figure S28: ^1H NMR of BSMImHSO$_4$. Figure S29: $^{13}C\{^1H\}$ NMR of BSMImHSO$_4$. Figure S30: ^1H NMR of BSMImBr. Figure S31: $^{13}C\{^1H\}$ NMR of BSMImBr. Figure S32: Conversion of Gly and products selectivity for the catalyst-free reaction between Gly and $HC(OMe)_3$ in function of the reaction time at room temperature and Q = 1. Figure S33: Conversion of Gly and products selectivity for the catalyst-free reaction between Gly and $HC(OMe)_3$ in function of the reaction time at room temperature and Q = 10. Figure S34: Conversion of Gly and and products selectivity for the reaction between $HC(OMe)_3$ and Gly in presence of Pyr-PTSA (10% w/wGly) in function of the reaction time at room temperature and Q = 10. Figure S35: GC-MS chromatograph of the reaction between $HC(OMe)_3$ and Gly (Q = 10, 90 °C, 24 h) in presence of sulfuric acid. Figure S36: MS spectra of the undefined compounds with retention time: 16.43 min. Figure S37: MS spectra of the undefined compounds with retention time: 16.59 min. Figure S38: MS

spectra of the undefined compounds with retention time: 16.43 min. Figure S39: MS spectra of the undefined compounds with retention time: 21.72 min.

Author Contributions: Conceptualization, A.P. and M.S.; Methodology, R.C.; Investigation, R.C. and E.A.; Data curation, E.A.; Writing—original draft preparation, R.C. and E.A.; Writing—review and editing, A.P. and M.S.; Supervision, A.P. and M.S.; Funding acquisition, M.S.

Abbreviations

Glyc	glycerol
OEs	orthoesters
Q	molar ratio $HC(OMe)_3$:glycerol
PPTS	pyridinium paratoluensulfonate
DBUHBr	diazabicycloundeconium bromide
A-15	Amberlyst 15
A-36	Amberlyst 36
$BSMIMHSO_4$	butylsulfonylmethylimidazolium hydrogensulfate
BSMIMBr	butylsulfonylmethylimidazolium bromide
$([P_{1888}]CH_3OCO_2^-)$	trioctylmethylphosphonium methylcarbonate

References

1.　Bozell, J.J.; Petersen, G.R. Technology development for the production of biobased products from biorefinery carbohydrates—The US Department of Energy's "Top 10" revisited. *Green Chem.* **2010**, *12*, 539–554. [CrossRef]

2.　Mota, C.J.; Pinto, B.P.; de Lima, A.L. *Glycerol*, 1st ed.; Springer: Berlin/Heidelberg, Germany, 2017; pp. 21–103.

3.　Hu, J.; Gu, Y.; Guan, Z.; Li, J.; Mo, W.; Li, T.; Li, G. An efficient palladium catalyst system for the oxidative carbonylation of glycerol to glycerol carbonate. *ChemSusChem* **2011**, *4*, 1767–1772. [CrossRef] [PubMed]

4.　Pearson, D.M.; Conley, N.R.; Waymouth, R.M. Palladium-catalyzed carbonylation of diols to cyclic carbonates. *Adv. Synth. Catal.* **2011**, *353*, 3007–3013. [CrossRef]

5.　Gabriele, B.; Mancuso, R.; Salerno, G. Oxidative carbonylation as a powerful tool for the direct synthesis of carbonylated heterocycles. *Eur. J. Org. Chem.* **2012**, *2012*, 6825–6839. [CrossRef]

6.　Casiello, M.; Monopoli, A.; Cotugno, P.; Milella, A.; Dell'Anna, M.M.; Ciminale, F.; Nacci, A. Copper (II) chloride-catalyzed oxidative carbonylation of glycerol to glycerol carbonate. *J. Mol. Catal. A Chem.* **2014**, *381*, 99–106. [CrossRef]

7.　Chavan, S.P.; Bhanage, B.M. Pd/C: An efficient and heterogeneous protocol for oxidative carbonylation of diols to cyclic carbonate. *Tetrahedron Lett.* **2014**, *55*, 1199–1202. [CrossRef]

8.　Guidi, S.; Calmanti, R.; Noè, M.; Perosa, A.; Selva, M. Thermal (catalyst-free) transesterification of diols and glycerol with dimethyl carbonate: A flexible reaction for batch and continuous-flow applications. *ACS Sustain. Chem. Eng.* **2016**, *4*, 6144–6151. [CrossRef]

9.　Calmanti, R.; Galvan, M.; Amadio, E.; Perosa, A.; Selva, M. High-temperature batch and continuous-flow transesterification of alkyl and enol esters with glycerol and its acetal derivatives. *ACS Sustain. Chem. Eng.* **2018**, *6*, 3964–3973. [CrossRef]

10.　Cattelan, L.; Perosa, A.; Riello, P.; Maschmeyer, T.; Selva, M. Continuous-flow o-alkylation of biobased derivatives with dialkyl carbonates in the presence of magnesium–aluminium hydrotalcites as catalyst precursors. *ChemSusChem* **2017**, *10*, 1571–1583. [CrossRef]

11.　Perosa, A.; Moraschini, A.; Selva, M.; Noè, M. Synthesis of the fatty esters of Solketal and glycerol-formal: Biobased specialty chemicals. *Molecules* **2016**, *21*, 170. [CrossRef]

12.　Guidi, S.; Noè, M.; Riello, P.; Perosa, A.; Selva, M. Towards a rational design of a continuous-flow method for the acetalization of crude glycerol: Scope and limitations of commercial amberlyst 36 and AlF3·3H2O as model catalysts. *Molecules* **2016**, *21*, 657. [CrossRef] [PubMed]

13.　Selva, M.; Guidi, S.; Noè, M. Upgrading of glycerol acetals by thermal catalyst-free transesterification of dialkyl carbonates under continuous-flow conditions. *Green Chem.* **2015**, *17*, 1008–1023. [CrossRef]

14. Cordes, E.; Bull, H. Mechanism and catalysis for hydrolysis of acetals, ketals, and ortho esters. *Chem. Rev.* **1974**, *74*, 581–603. [CrossRef]

15. Greene, T.W.; Wuts, P.G.M. *Protective Groups in Organic Synthesis*, 4th ed.; Wiley: New York, NY, USA, 2014.

16. Kociensky, P.J. *Protecting Groups*, 3rd ed.; Thieme-Verlag: New York, NY, USA, 2005.

17. Gabriele, B.; Mancuso, R.; Salerno, G.; Veltri, L.; Costa, M.; Dibenedetto, A. A general and expedient synthesis of 5- and 6-membered cyclic carbonates by palladium-catalyzed oxidative carbonylation of 1, 2- and 1, 3-diols. *ChemSusChem* **2011**, *4*, 1778–1786. [CrossRef] [PubMed]

18. Zhou, X.; Luo, S.; Tang, R.; Wang, R.; Wang, J. Diblock copolymers of polyethylene glycol and a polymethacrylamide with side-chains containing twin ortho ester rings: Synthesis, characterization, and evaluation as potential pH-responsive micelles. *Macromol. Biosci.* **2015**, *15*, 385–394. [CrossRef] [PubMed]

19. Heller, J.; Barr, J. Poly(ortho esters) from concept to reality. *Biomacromolecules* **2004**, *5*, 1625–1632. [CrossRef] [PubMed]

20. Brachvogel, R.-C.; Hampel, F.; Von Delius, M. Self-assembly of dynamic orthoester cryptates. *Nat. Commun.* **2015**, *6*, 7129. [CrossRef] [PubMed]

21. Löw, H.; Mena-Osteritz, E.; von Delius, M. Self-assembled orthoester cryptands: Orthoester scope, post-functionalization, kinetic locking and tunable degradation kinetics. *Chem. Sci.* **2018**, *9*, 4785–4793. [CrossRef] [PubMed]

22. Crank, G.; Eastwod, F. Derivatives of orthoacids. I. Bicyclic orthoesters. *Aust. J. Chem.* **1964**, *17*, 1385–1391. [CrossRef]

23. Crank, G.; Eastwood, F. Derivatives of orthoacids. II. The preparation of olefins from 1, 2-diols. *Aust. J. Chem.* **1964**, *17*, 1392–1398. [CrossRef]

24. Tshibalonza, N.N.; Monbaliu, J.-C.M. Revisiting the deoxydehydration of glycerol towards allyl alcohol under continuous-flow conditions. *Green Chem.* **2017**, *19*, 3006–3013. [CrossRef]

25. Hall, H., Jr.; DeBlauwe, F.; Pyriadi, T. 2,6,7-Trioxabicyclo[2.2.1]heptane. *J. Am. Chem. Soc.* **1975**, *97*, 3854. [CrossRef]

26. Yokoyama, Y.; Padias, A.B.; De Blauwe, F.; Hall, H., Jr. Synthesis and polymerization of 2, 6, 7-trioxabicyclo[2.2.1]heptane and 1-Methyl-2, 6, 7-trioxabicyclo [2.2.1]heptane. *Macromolecules* **1980**, *13*, 252–261. [CrossRef]

27. Heller, J.; Barr, J.; Ng, S.Y.; Abdellauoi, K.S.; Gurny, R. Poly (ortho esters): Synthesis, characterization, properties and uses. *Adv. Drug Del. Rev.* **2002**, *54*, 1015–1039. [CrossRef]

28. Padias, A.B.; Szymanski, R.; Hall, H.K. Synthesis and polymerization of atom-bridged bicyclic acetals and ortho esters. In *Ring-Opening Polymerization*; American Chemical Society: Washington, DC, USA, 1985; Volume 286, pp. 313–333.

29. Yokoyama, Y.; Hall, H. Ring-opening polymerization of atom-bridged and bond-bridged bicyclic ethers, acetals and orthoesters. In *New Polymerization Reactions*; Springer: Berlin/Heidelberg, Germany, 1982; pp. 107–138.

30. Zhang, L.; Yu, M.; Wang, J.; Tang, R.; Yan, G.; Yao, W.; Wang, X. Low molecular weight PEI-based vectors via acid-labile ortho ester linkage for improved gene delivery. *Macromol. Biosci.* **2016**, *16*, 1175–1187. [CrossRef] [PubMed]

31. Amarasekara, A.S. Acidic ionic liquids. *Chem. Rev.* **2016**, *116*, 6133–6183. [CrossRef]

32. Cox, J. A bond energy scheme—II: Strain and conjugation energies in cyclic compounds. *Tetrahedron* **1963**, *19*, 1175–1184. [CrossRef]

33. Fletcher, S.E.; Mortimer, C.T.; Springall, H.D. 118. Heats of combustion and molecular structure. Part VII. 1:3-Dioxane and 1:3:5-trioxa-cycloalkenes. *J. Chem. Soc.* **1959**, 580–584. [CrossRef]

34. Brachvogel, R.-C.; von Delius, M. Orthoester exchange: A tripodal tool for dynamic covalent and systems chemistry. *Chem. Sci.* **2015**, *6*, 1399–1403. [CrossRef]

35. Kaupmees, K.; Trummal, A.; Leito, I. Basicities of strong bases in water: A computational study. *Croat. Chem. Acta* **2014**, *87*, 385–395. [CrossRef]

36. Mezheritskii, V.V.; Olekhnovich, E.P.; Dorofeenko, G.N. The properties of orthoesters and their applications in organic synthesis. *Russ. Chem. Rev.* **1973**, *42*, 392. [CrossRef]

37. Cordes, H. Ortho esters. In *Carboxylic Acids and Esters*; Patai, S., Ed.; Wiley: Hoboken, NJ, USA, 1969.

38. Fabris, M.; Lucchini, V.; Noè, M.; Perosa, A.; Selva, M. Ionic liquids made with dimethyl carbonate: solvents as well as boosted basic catalysts for the Michael reaction. *Chem. Eur. J.* **2009**, *15*, 12273–12282. [CrossRef] [PubMed]

39. Thomazeau, C.; Olivier-Bourbigou, H.; Magna, L.; Luts, S.; Gilbert, B. Determination of an acidic scale in room temperature ionic liquids. *J. Chem. Soc.* **2003**, *125*, 5264–5265. [CrossRef] [PubMed]

40. Tao, D.-J.; Wu, J.; Wang, Z.-Z.; Lu, Z.-H.; Yang, Z.; Chen, X.-S. SO$_3$H-functionalized Brønsted acidic ionic liquids as efficient catalysts for the synthesis of isoamyl salicylate. *RSC Adv.* **2014**, *4*, 1–7. [CrossRef]

41. Olah, A.; Prakash, G.K.S.; Sommer, J. *Superacids*; Wiley: Chichester, UK, 1985.

42. Bringué, R.; Iborra, M.; Tejero, J.; Izquierdo, J.F.; Cunill, F.; Fité, C.; Cruz, V.J. Thermally stable ion-exchange resins as catalysts for the liquid-phase dehydration of 1-pentanol to di-n-pentyl ether (DNPE). *J. Catal.* **2006**, *244*, 33–42. [CrossRef]

43. Harmer, M.A.; Sun, Q. Solid acid catalysis using ion-exchange resins. *Appl. Catal. Gen.* **2001**, *221*, 45–62. [CrossRef]

44. Ni, L.; Xin, J.; Jiang, K.; Chen, L.; Yan, D.; Lu, X.; Zhang, S. One-step conversion of biomass-derived furanics into aromatics by Brønsted acid ionic liquids at room temperature. *ACS Sustain. Chem. Eng.* **2018**, *6*, 2541–2551. [CrossRef]

45. Yao, L.; Liu, S.; Li, L.; Yu, S.; Liu, F.; Song, Z. Synthesis of hydroxymethylfurfural from sucrose using brönsted-lewis acidic ionic liquid. *Bull. Chem. Soc. Ethiop.* **2016**, *30*, 283–286. [CrossRef]

46. Miyashita, M.; Yoshikoshi, A.; Grieco, P.A. Pyridinium p-toluenesulfonate. A mild and efficient catalyst for the tetrahydropyranylation of alcohols. *J. Org. Chem.* **1977**, *42*, 3772–3774. [CrossRef]